

Controlling stationary one-way steering in a three-level atomic ensemble

Jie Peng(彭洁), Jun Xu(徐俊), Hua-Zhong Liu(刘华忠), and Zhang-Li Lai(赖章丽)
Citation: Chin. Phys. B, 2023, 32 (**12**): 120305. DOI: 10.1088/1674-1056/acf82b
Journal homepage: http://cpb.iphy.ac.cn; http://iopscience.iop.org/cpb

What follows is a list of articles you may be interested in

Generation of hyperentangled photon pairs based on lithium niobate waveguide

Yang-He Chen(陈洋河), Zhen Jiang(姜震), and Guang-Qiang He(何广强)
Chin. Phys. B, 2023, 32 (**9**): 090306. DOI: 10.1088/1674-1056/acd5c4

Commensurate and incommensurate Haldane phases for a spin-1 bilinear-biquadratic model

Yan-Wei Dai(代艳伟), Ai-Min Chen(陈爱民), Xi-Jing Liu(刘希婧), and Yao-Heng Su(苏耀恒)
Chin. Phys. B, 2023, 32 (**9**): 090304. DOI: 10.1088/1674-1056/acac0c

Degenerate polarization entangled photon source based on a single Ti-diffusion lithium niobate waveguide in a polarization Sagnac interferometer

Yu Sun(孙宇), Chang-Wei Sun(孙昌伟), Wei Zhou(周唯), Ran Yang(杨然), Jia-Chen Duan(端家晨), Yan-Xiao Gong(龚彦晓), Ping Xu(徐平), and Shi-Ning Zhu(祝世宁)
Chin. Phys. B, 2023, 32 (**8**): 080308. DOI: 10.1088/1674-1056/acd8b3

First-order quantum phase transition and entanglement in the Jaynes-Cummings model with a squeezed light

Chun-Qi Tang(汤椿琦) and Li-Tuo Shen(沈利托)
Chin. Phys. B, 2023, 32 (**7**): 070303. DOI: 10.1088/1674-1056/acb9f0

Faithful and efficient hyperentanglement purification for spatial-polarization-time-bin photon system

Fang-Fang Du(杜芳芳), Gang Fan(樊钢), Yi-Ming Wu(吴一鸣), and Bao-Cang Ren(任宝藏)
Chin. Phys. B, 2023, 32 (**6**): 060304. DOI: 10.1088/1674-1056/aca395

Controlling stationary one-way steering in a three-level atomic ensemble

Jie Peng(彭洁)[1], Jun Xu(徐俊)[2,†], Hua-Zhong Liu(刘华忠)[1], and Zhang-Li Lai(赖章丽)[3]

[1] *Department of Basic Courses, Wuhan Donghu University, Wuhan* 430071, *China*
[2] *College of Physical Science and Technology, Central China Normal University, Wuhan* 430079, *China*
[3] *College of Mathematics and Physics, Jinggangshan University, Ji'an* 343009, *China*

(Received 3 June 2023; revised manuscript received 7 September 2023; accepted manuscript online 9 September 2023)

We propose a scheme for establishing the stationary one-way quantum steering in a three-level Λ-type atomic ensemble. In our system, the cavity modes are generated from two atomic dipole-allowed transitions, which are in turn driven by two external classical fields. The atomic ensemble can act as an engineered reservoir to put two cavity modes into a squeezed state by two Bogoliubov dissipation pathways. When the damping rates of the two cavity modes are different, the steady-state one-way quantum steering of the intracavity and output fields is presented by adjusting the normalized detuning. The physical mechanism is analyzed based on a dressed state representation and Bogoliubov mode transformation. The achieved optical one-way quantum steering scheme has potential applications in quantum secret information sharing protocols.

Keywords: one-way quantum steering, entanglement, quantum correlation, reservoir-engineered method

PACS: 03.67.Bg, 42.50.Dv, 42.50.Pq, 32.80.Qk **DOI:** 10.1088/1674-1056/acf82b

1. Introduction

Ever since Einstein, Podolsky and Rosen (EPR) demonstrated that measuring one of a pair of quantum-entangled particles instantaneously affects the other, regardless of their physical separation, it has been observed that these particles can exist in two distinct states simultaneously.[1] In 1935, Schrödinger introduced the concept of steering to provide a broader framework for understanding the strange phenomenon of action at a distance.[2] Wiseman *et al.* showed that EPR steering can be described as a new kind of quantum correlation, which is stronger than entanglement but weaker than Bell nonlocality.[3] This suggests that quantum steering can transition from being a conceptual idea to a quantifiable theoretical and experimental reality. A violation of the Bell inequality means that a quantum bipartite state can exhibit steering in both directions. EPR steering is inherently distinct from entanglement and Bell nonlocality, i.e., one-way EPR steering.[4–8] Asymmetric one-way quantum steering is demonstrated as a situation in which Alice can steer Bob but Bob cannot steer Alice, or vice versa.[9,10] This unique feature has attracted significant attention and is widely used in practical applications, such as directional recessive conduction, one-side device-independent quantum cryptography, quantum teleportation and high-fidelity heralded teleportation.[11–14] Many different criteria based on the uncertainty principle have been proposed to decide whether a quantum state is steerable. Reid put forward the criterion of a continuous variable Gaussian state.[15] Wiseman *et al.* raised a criterion applicable to discrete and continuous variables.[3] Walborn *et al.* presented a generalized entropy criterion for the continuous variable non-Gaussian state.[16–18] Ioannis Kogias *et al.* introduced a computable measure of steering for arbitrary bipartite Gaussian states.[19] In addition to the relevant theoretical advances,[15–21] quantum steering experiments have also made great progress.[5,22–29] For example, Handchen *et al.* observed one-way EPR steering of two-mode Gaussian squeezed states for the first time.[27] Armstrong *et al.* showed multipartite EPR steering and genuine tripartite entanglement with optical networks.[22] Xiao *et al.* experimentally demonstrated one-way EPR steering with multimeasurement settings for a class of two-qubit states, which are still one-way steerable even with infinite settings,[29] and so on.

One-way EPR steering plays an important role in quantum information and fundamental physics. Over the past decades, much work has been devoted to finding effective ways to test the quantum effect in atomic systems,[30–35] such as quantum jumps in atomic systems,[30] strong coupling of optical nanoantennas and atomic systems,[32] and weak-interaction effects in heavy atomic systems.[33] Many schemes for quantum steering based on atomic systems have been proposed.[36–42] For instance, Xu *et al.* employed a two-level atomic ensemble driven by a strong laser field inside a two-mode cavity and showed a significant enhancement of the output steady-state quantum correlations via a dissipative atomic reservoir. On the condition of an unbalanced coupling strength, asymmetrical output one-way EPR steering has been achieved.[37] Tan *et al.* proposed a scheme for realizing hybrid atom-mechanical quantum steering in the steady-state regime. An optomechanical two-mode cavity was coupled to a distant ensemble of double-Λ atoms in a cascade setup, leading to a

†Corresponding author. E-mail: junxu@ccnu.edu.cn

© 2023 Chinese Physical Society and IOP Publishing Ltd

dissipative interaction between the mechanics and the internal atomic states.[38] He *et al.* studied multipartite entanglement, the generation of EPR states and quantum steering in a three-mode optomechanical system composed of an atomic ensemble located inside a single-mode cavity with a movable mirror. Two-way EPR steering was found between the mirror and the atomic ensemble despite the fact that they were not directly coupled to each other.[39]

Here, we present a scheme for generating tunable asymmetric quantum steering in a three-level Λ-type atomic system. The cavity modes are generated from two atomic dipole-allowed transitions, which are driven by two external classical fields, respectively. When two cavity modes are tuned to be resonant with Rabi sidebands of the dressed atom, two collective Bogoliubov modes formed by the original cavity modes interact effectively with the dressed atom. The atomic ensemble, which serves as an engineered reservoir, can cool two Bogoliubov modes into a vacuum state. At this moment, the original cavity modes reach a squeezing state. It is because of the two Bogoliubov dissipation pathways that entanglement is greatly enhanced. The best obtained state tends to be the original EPR entangled state. By adjusting the normalized detuning and the cavity damping rates, steady-state one-way quantum steering of the intracavity and output fields can be achieved. To describe the physical process more clearly, the dressed state representation[46] and Bogoliubov transformation[47] have been used. Compared with other schemes, our scheme has the following features: (i) A four-wave mixing process in the three-level atomic system is used to generate the entangled light.[43–45] This is very easy to implement experimentally. (ii) The obtained asymmetric quantum steering by two Bogoliubov dissipation pathways is robust against environmental noise and does not require the initial preparation of nonclassical states. (iii) The direction of the one-way quantum steering can be easily controlled by adjusting the normalized detuning and the cavity damping rates.

The rest of this article is organized as follows. In Section 2, we describe the system model and present the interaction equations. In Section 3, we discuss one-way EPR steering and entanglement of intracavity fields, and then analyze the physical mechanism. The output steering and entanglement are given in Section 4. The article ends with a conclusion in Section 5.

2. Model and equations

As sketched in Fig. 1(a), an ensemble of three-level Λ atoms placed at the intersection of two cavities is driven by two external pumping fields with Rabi frequencies Ω_1 and Ω_2. This atomic ensemble has a ground state $|1\rangle$, a metastable state $|2\rangle$ and an excited state $|3\rangle$, as shown in Fig. 1(b). A large number of atomic structures can be used as candidates, for example, the rubidium 87 D_1 transition, $|1\rangle = |5^2S_{1/2}, F = 1\rangle$, $|2\rangle = |5^2S_{1/2}, F = 2\rangle$ and $|3\rangle = |5^2P_{1/2}, F = 1\rangle$. The pumping field with Ω_1 drives atoms from the ground state $|1\rangle$ to the virtual energy level below the excited state $|3\rangle$. Since the virtual level is an unstable state, it will emit a photon of a_2 back to the virtual energy level above the ground state $|2\rangle$. Then it absorbs a pumping photon of Ω_2 and emits a photon of a_1. This is commonly known as the four-wave mixing process. In this case, energy and momentum conservation conditions must be satisfied, i.e., $\omega_1 + \omega_2 = \nu_1 + \nu_2$ and $\boldsymbol{k}_{\omega_1} + \boldsymbol{k}_{\omega_2} = \boldsymbol{k}_{\nu_1} + \boldsymbol{k}_{\nu_2}$. ω_l is the corresponding driving field frequency, ν_l is the cavity field frequency and $\boldsymbol{k}_{\omega_l,\nu_l}$ is the corresponding wave vector.

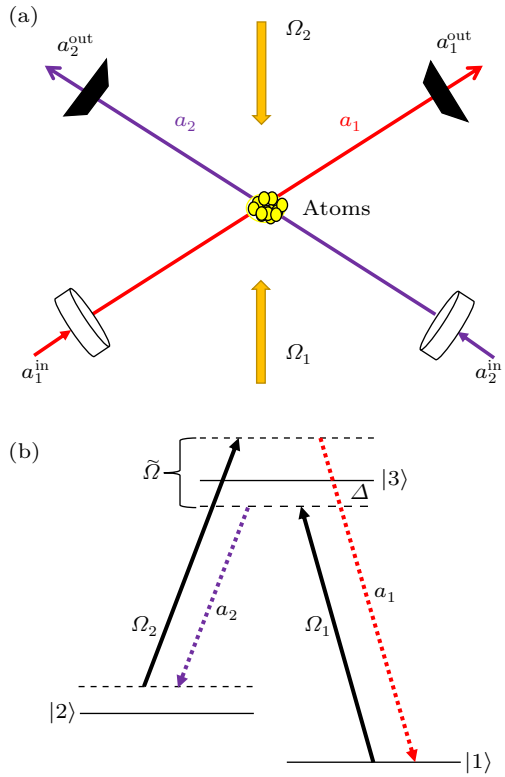


Fig. 1. (a) An ensemble of Λ-type atoms are placed at the intersection of two cavities driven by two external coherent fields with half Rabi frequencies $\Omega_{1,2}$ (b) The bare atomic states and transitions in Λ configuration. $\Omega_{1,2}$ are applied to the atomic transitions $|1,2\rangle \to |3\rangle$, and separately tuned from the atomic transitions by $\Delta_1 = -\Delta_2 = \Delta$. Two cavity fields $a_{1,2}$ are detuned from the driving field frequencies by $\tilde{\Omega}$, where $\tilde{\Omega}$ is the spacing between adjacent dressed states.

In the dipole approximation and an appropriate rotating frame, the master equation for the atom-field density operator ρ is written as

$$\frac{\mathrm{d}}{\mathrm{d}t}\rho = -\frac{\mathrm{i}}{\hbar}[H,\rho] + \sum_{l=1}^{2}(\gamma_l \mathcal{L}_{\sigma_{l3}}\rho + \kappa_l \mathcal{L}_{a_j}\rho) \tag{1}$$

with $H = H_0 + H_{\rm I}$, where

$$H_0 = \sum_{l=1}^{2}\hbar[-\Delta_l\sigma_{ll} + \Omega_l(\sigma_{3l} + \sigma_{l3})] \tag{2}$$

describes the interaction of the three-level atoms with the driving fields and

$$H_{\rm I} = \sum_{l=1}^{2}\hbar[\delta_l a_l^{\dagger}a_l + g_l(\sigma_{3l}a_l + a_l^{\dagger}\sigma_{l3})] \tag{3}$$

represents the interaction between the atoms and the cavity fields. $\sigma_{mn}=\sum_{\mu=1}^{N}\sigma_{mn}^{\mu}$ ($\sigma_{mn}^{\mu}=|m^{\mu}\rangle\langle n^{\mu}|$; $m,n=1,2,3$) denotes collective projection operator of N independent atoms for $m=n$ and collective spin-flip operator for $m\neq n$. a_l and $a_l^{\dagger}$ represent annihilation and creation operators of the lth cavity field, and g_l denotes the coupling strength of the atoms with the lth cavity field. $\Delta_l=\omega_{3l}-\omega_l$ and $\delta_l=\nu_l-\omega_l$ are the detunings of the atomic resonance frequency ω_{3l} and the lth cavity field frequency ν_l with respect to the corresponding driving field frequencies ω_l. The second and the third terms in Eq. (1) describe atomic spontaneous emission decays with rates γ_l and cavity damping rates κ_l, in which $\mathcal{L}_o\rho=(1/2)(2o\rho o^{\dagger}-\rho o^{\dagger}o-o^{\dagger}o\rho)$.

Next, we transform the atomic variables into a dressed-state representation. For simplicity, we take the antisymmetrical tuning $\Delta_1=-\Delta_2=\Delta$ and the same Rabi sidebands $\Omega_1=\Omega_2=\Omega$. We assume that the Rabi frequency is real and much stronger than the atomic decays and cavity losses $\Omega\gg g_l\langle a_l\rangle$, γ_l, κ_l. By diagonalizing the Hamiltonian H_0, the dressed states are expressed as

$$\begin{aligned}
|+\rangle&=\frac{1+\sin\theta}{2}|1\rangle+\frac{1-\sin\theta}{2}|2\rangle+\frac{\cos\theta}{2}|3\rangle,\\
|0\rangle&=-\frac{\cos\theta}{2}|1\rangle+\frac{\cos\theta}{2}|2\rangle+\frac{\sin\theta}{2}|3\rangle,\\
|-\rangle&=\frac{1-\sin\theta}{2}|1\rangle+\frac{1+\sin\theta}{2}|2\rangle-\frac{\cos\theta}{2}|3\rangle,
\end{aligned}\tag{4}$$

where $\sin\theta=\Delta/\tilde{\Omega}$, $\cos\theta=\sqrt{2}\Omega/\tilde{\Omega}$, and $\tilde{\Omega}=\sqrt{\Delta^2+2\Omega^2}$ denotes energy splitting of the dressed states. The dressed states $|0\rangle$, $|+\rangle$ and $|-\rangle$ have eigenvalues $\lambda_{0,\pm}=0,\pm\tilde{\Omega}$, respectively. The free Hamiltonian H_0 becomes $H_0'=\hbar\tilde{\Omega}(\sigma_{++}-\sigma_{--})$, where $\sigma_{jk}=\sum_{\mu=1}^{N}|j^{\mu}\rangle\langle k^{\mu}|$, $(j,k=0,\pm)$ are the projection operators ($j=k$) and the flip operators ($j\neq k$) of the ensemble in terms of the dressed states. The damping rates in terms of the dressed states are given in Appendix A. The steady-state populations ($N_j=\langle\sigma_{jj}\rangle$) of the dressed states in the absence of cavity fields are calculated as $N_0=\frac{N\cos^4\theta}{1+3\sin^4\theta}$ and $N_{\pm}=(N-N_0)/2$.

The cavity fields are tuned to be resonant with dressed atomic Rabi sidebands, i.e., $\delta_1=-\delta_2=\tilde{\Omega}$. Making a unitary transformation with $U'=\exp(-\mathrm{i}\hat{H}_0't/\hbar)$ and neglecting rapidly oscillating terms such as $\exp\pm(\mathrm{i}\tilde{\Omega}t)$ and $\exp\pm(2\mathrm{i}\tilde{\Omega}t)$, the master equation $\hat{\rho}'=U'^{\dagger}\hat{\rho}U'$ has the same form as that in Eq. (1) by taking the following Hamiltonian:

$$H_{\mathrm{I}}'=\hbar(g_{11}a_1+g_{22}a_2^{\dagger})\sigma_{+0}+\hbar(g_{21}a_2+g_{12}a_1^{\dagger})\sigma_{-0}+\mathrm{H.c.}\tag{5}$$

with $g_{11}=-g_1\cos^2\theta/2$, $g_{12}=g_1\sin\theta(1-\sin\theta)/2$, $g_{21}=-g_2\cos^2\theta/2$, $g_{22}=g_2\sin\theta(1-\sin\theta)/2$. Physically, it is easy to find that the transition $|0\rangle\rightarrow|+\rangle$ is accompanied by the absorption of an a_1 photon and the emission of an a_2 photon. Correspondingly, the transition $|0\rangle\rightarrow|-\rangle$ is accompanied by the emission of an a_1 photon and the absorption of an a_2 photon.

Quantum correlations can be calculated by following the standard technique.[48] From the master equation, we derive the set of linearized Langevin equations for the operators $\delta o=o-\langle o\rangle$ as follows:

$$\begin{aligned}
\dot{a}_1&=-\frac{\kappa_1}{2}a_1-\mathrm{i}g_{11}\sigma_{0+}-\mathrm{i}g_{12}\sigma_{-0}+\sqrt{\kappa_1}a_1^{\mathrm{in}}(t),\\
\dot{a}_2&=-\frac{\kappa_2}{2}a_2-\mathrm{i}g_{22}\sigma_{+0}-\mathrm{i}g_{21}\sigma_{0-}+\sqrt{\kappa_2}a_2^{\mathrm{in}}(t),\\
\dot{\sigma}_{0+}&=-\frac{\Gamma_1}{2}\sigma_{0+}-\mathrm{i}g_{11}N_{0+}a_1-\mathrm{i}g_{22}N_{0+}a_2^{\dagger}+\gamma_{\mathrm{c}2}\sigma_{-0}\\
&\quad+F_{\sigma_{0+}}(t),\\
\dot{\sigma}_{0-}&=-\frac{\Gamma_2}{2}\sigma_{0-}-\mathrm{i}g_{12}N_{0-}a_1^{\dagger}-\mathrm{i}g_{21}N_{0-}a_2+\gamma_{\mathrm{c}1}\sigma_{+0}\\
&\quad+F_{\sigma_{0-}}(t),
\end{aligned}\tag{6}$$

where $N_{0\pm}=N_0-N_{\pm}$ represents the dressed population difference. $\Gamma_{1,2}$ are the collective damping rates between $|\pm\rangle$ and $|0\rangle$, which can be found in Appendix A. Note that the symbol δ is omitted from now on because the expected values of these operators are $\langle o\rangle=0$ in our schemes. The noise operators a_j^{in} satisfy the nonzero correlations $\langle a_j^{\mathrm{in}}(t)a_{j'}^{\mathrm{in}\dagger}(t')\rangle=\delta_{jj'}\delta(t-t')$. The F's are the atomic noise terms with zero means and correlations $\langle F_o(t)F_{o'}(t')\rangle=2D_{oo'}\delta(t-t')$, where the nonzero diffusion coefficients $2D_{\sigma_{0+}\sigma_{+0}}=\Gamma_1N_0$, $2D_{\sigma_{+0}\sigma_{0+}}=\Gamma_1N_+$, $2D_{\sigma_{0-}\sigma_{-0}}=\Gamma_2N_0$, $2D_{\sigma_{-0}\sigma_{0-}}=\Gamma_2N_-$, $2D_{\sigma_{0+}\sigma_{0-}}=2D_{\sigma_{-0}\sigma_{+0}}=-\gamma_{\mathrm{c}1}N_0-\gamma_{\mathrm{c}2}N_-$, $2D_{\sigma_{+0}\sigma_{-0}}=2D_{\sigma_{0-}\sigma_{0+}}=-\gamma_{\mathrm{c}1}N_+-\gamma_{\mathrm{c}2}N_0$.

Utilizing the standard method proposed in Ref. [49] and arranging the operators as a column vector $\psi=(a_1,a_1^{\dagger},a_2,a_2^{\dagger},\sigma_{0+},\sigma_{+0},\sigma_{0-},\sigma_{-0})^{\mathrm{T}}$, we can simplify Eq. (6) as

$$\frac{\mathrm{d}}{\mathrm{d}t}\psi(t)=\boldsymbol{R}\psi(t)-\sqrt{\boldsymbol{Q}}\psi_{\mathrm{in}}(t),\tag{7}$$

where $\boldsymbol{Q}=\mathrm{diag}(\kappa_1,\kappa_1,\kappa_2,\kappa_2,1,1,1,1)$, $\psi_{\mathrm{in}}=(a_1^{\mathrm{in}},a_1^{\mathrm{in}\dagger},a_2^{\mathrm{in}},a_2^{\mathrm{in}\dagger},F_{\sigma_{0+}},F_{\sigma_{+0}},F_{\sigma_{0-}},F_{\sigma_{-0}})^{\mathrm{T}}$ and $\boldsymbol{R}$ is an 8×8 drift matrix. The formal solutions of Eq. (7) are

$$\begin{aligned}
\psi(t)&=\mathrm{e}^{\boldsymbol{R}t}\psi(0)-\sqrt{\boldsymbol{Q}}\int_0^t\psi_{\mathrm{in}}(t')\mathrm{e}^{\boldsymbol{R}(t-t')}\mathrm{d}t',\\
\psi^{\mathrm{T}}(t)&=\mathrm{e}^{\boldsymbol{R}^{\mathrm{T}}t}\psi^{\mathrm{T}}(0)-\sqrt{\boldsymbol{Q}}\int_0^t\psi_{\mathrm{in}}^{\mathrm{T}}(t')\mathrm{e}^{\boldsymbol{R}^{\mathrm{T}}(t-t')}\mathrm{d}t'.
\end{aligned}$$

To study the quantum correlations, the second-order moments $\Phi=\langle\psi(t)\psi^{\mathrm{T}}(t)\rangle$ take the following form:

$$\frac{\mathrm{d}}{\mathrm{d}t}\Phi=\boldsymbol{R}\Phi+\Phi\boldsymbol{R}^{\mathrm{T}}+\boldsymbol{Q}\cdot\boldsymbol{D},\tag{8}$$

where $\boldsymbol{D}$ is an 8×8 correlation matrix, which can be written as

$$\boldsymbol{D}=\begin{pmatrix}
0&1&0&0&0&0&0&0\\
0&0&0&0&0&0&0&0\\
0&0&0&1&0&0&0&0\\
0&0&0&0&0&0&0&0\\
0&0&0&0&0&\Gamma_1N_0&-\gamma_{\mathrm{c}1}'&0\\
0&0&0&0&\Gamma_1N_+&0&0&-\gamma_{\mathrm{c}2}'\\
0&0&0&0&-\gamma_{\mathrm{c}2}'&0&0&\Gamma_2N_0\\
0&0&0&0&0&-\gamma_{\mathrm{c}1}'&\Gamma_2N_-&0
\end{pmatrix},\tag{9}$$

where $\gamma'_{c1} = \gamma_{c1}N_0 + \gamma_{c2}N_-$ and $\gamma'_{c2} = \gamma_{c1}N_+ + \gamma_{c2}N_0$. The steady-state solution of the second-order moments can be obtained from Eq. (9).

In order to calculate the quantum correlations between the two modes, it is desirable that the system should be stable. According to the Routh–Hurwitz criterion,[50–52] the stability conditions of the system can be calculated to be

$$\begin{aligned} S_1 &= \Gamma^2\kappa + \Gamma\kappa^2 - 4\kappa\gamma_{c1}^2 - 2N_{0+}G_1(\Gamma+\kappa) > 0, \\ S_2 &= \Gamma^3 + 4\Gamma^2\kappa + 4\Gamma\kappa^2 - 4\Gamma\gamma_{c1}^2 + \kappa^3 \\ &\quad - 2N_{0+}G_1(\Gamma+\kappa) > 0, \\ S_1S_2 &> -\frac{1}{2}(\Gamma+\kappa)^2[16N_{0+}^2G_2 - 2N_{0+}G_1\Gamma\kappa \\ &\quad + (\Gamma^2 - 4\gamma_{c1}^2)\kappa^2], \end{aligned} \tag{10}$$

where we have defined $G_1 = g_{11}^2 - g_{12}^2 + g_{21}^2 - g_{22}^2$, $G_2 = (g_{11}g_{21} - g_{12}g_{22})^2$, and have assumed $\gamma_1 = \gamma_2 = \gamma$, $\kappa_1 = \kappa_2 = \kappa$, and $\Gamma_1 = \Gamma_2 = \Gamma$ for simplification.

3. Quantum steering and entanglement of intracavity fields

In this section, we investigate the properties of stationary quantum steering for the intracavity fields and analyze how to obtain one-way quantum steering by controlling the normalized detuning and choosing an appropriate ratio of two cavity losses. For the present mixed system, assuming that the cavity modes are initially in vacuum, the cavity-field states should be in a two-mode Gaussian state. The operators X_j and Y_j $(j = 1,2)$ are a pair of quadrature operators defined as $X_j = (a_j + a_j^\dagger)/\sqrt{2}$ and $Y_j = -\mathrm{i}(a_j - a_j^\dagger)/\sqrt{2}$. Defining $\xi = (X_1, Y_1, X_2, Y_2)$, the quantum statistical properties of a two-mode Gaussian state are determined by its correlation matrix $\boldsymbol{CM}_{ij} = \langle \xi_i\xi_j + \xi_j\xi_i\rangle/2$. This matrix can be written as $\boldsymbol{CM} = \begin{pmatrix} \boldsymbol{T}_1 & \boldsymbol{T}_3 \\ \boldsymbol{T}_3^{\mathrm{T}} & \boldsymbol{T}_2 \end{pmatrix}$, where $\boldsymbol{T}_1 = \begin{pmatrix} n_1 & 0 \\ 0 & n_1 \end{pmatrix}$, $\boldsymbol{T}_2 = \begin{pmatrix} n_2 & 0 \\ 0 & n_2 \end{pmatrix}$, $\boldsymbol{T}_3 = \begin{pmatrix} c & 0 \\ 0 & -c \end{pmatrix}$. Here, $n_j = \langle a_j^\dagger a_j\rangle_{\mathrm{ss}} + \frac{1}{2}$, $c = \langle a_1 a_2\rangle_{\mathrm{ss}}$, which are determined by the steady-state solution of Eq. (9).

As usual, the entanglement degree of the two-mode cavity field can be quantified with logarithmic negativity E_{N}. For the two-mode Gaussian state, the logarithmic negativity E_{N} can be calculated by defining[53–55]

$$E_{\mathrm{N}} = \max[0, -\ln 2\eta^-], \tag{11}$$

where $\eta^- = 2^{-1/2}\sqrt{\Sigma - \sqrt{\Sigma^2 - 4\det\boldsymbol{CM}}}$ and $\Sigma = \det\boldsymbol{T}_1 + \det\boldsymbol{T}_2 - 2\det\boldsymbol{T}_3$. According to Ref. [19], the proposed measurement of the Gaussian quantum steerability in the $a_1 \to a_2$ direction is given as

$$\mathcal{G}_{\mathrm{A}} \equiv \mathcal{G}_{a_1\to a_2}(\boldsymbol{CM}) = \max\left[0, \frac{1}{2}\ln\frac{\boldsymbol{T}_1}{4\boldsymbol{CM}}\right], \tag{12}$$

and the steering measurement in the direction $a_2 \to a_1$ can be obtained by swapping a_1 and a_2,

$$\mathcal{G}_{\mathrm{B}} \equiv \mathcal{G}_{a_2\to a_1}(\boldsymbol{CM}) = \max\left[0, \frac{1}{2}\ln\frac{\boldsymbol{T}_2}{4\boldsymbol{CM}}\right]. \tag{13}$$

Here we introduce the steering asymmetry defined as $|\mathcal{G}_{\mathrm{A}} - \mathcal{G}_{\mathrm{B}}|$ in order to check the asymmetric steerability of the two-mode Gaussian states.

Figure 2 shows the intracavity entanglement E_{N} (black solid line), the intracavity steering $\mathcal{G}_{\mathrm{A}}$ (red dashed line), $\mathcal{G}_{\mathrm{B}}$ (blue dot-dashed line) and the steering asymmetry $|\mathcal{G}_{\mathrm{A}} - \mathcal{G}_{\mathrm{B}}|$ (green dotted line) versus the normalized detuning Δ/Ω for different cavity loss rate ratios κ_1/κ_2: (a) $\kappa_1/\kappa_2 = 1$, (b) $\kappa_1/\kappa_2 = 3$, (c) $\kappa_1/\kappa_2 = 4$, (d) $\kappa_1/\kappa_2 = 16$. The other parameters are chosen as $\gamma_1 = \gamma_2 = 1$, $\kappa_2 = 0.1$, $g_1\sqrt{N} = g_2\sqrt{N} = 5$. When the absolute value $|\Delta|/\Omega$ of the normalized detuning decreases, there will be two competing effects. On the one hand, it can increase the effective coupling $\hbar\sqrt{g_{\mathrm{a}}^2 - g_{\mathrm{b}}^2}$. On the other hand, it will decrease the squeezing parameter r. The effective coupling and squeezing parameters are given at the end of this section. Therefore, entanglement and steering are nonmonotonic functions of Δ/Ω and take a maximum close to the infinite squeezing parameter r, i.e., $\Delta/\Omega \to -0.8164$. It can be found that the optimal values of both steering and entanglement gradually decrease with the increase of the cavity loss rate κ_1. Specifically, when the cavity loss rate κ_1 is large enough, e.g., $\kappa_1/\kappa_2 = 4$, the $a_1 \to a_2$ steering $\mathcal{G}_{\mathrm{A}}$ disappears completely, while there is still $a_2 \to a_1$ steering $\mathcal{G}_{\mathrm{B}}$. As the cavity loss rate κ_1 continues to increase, the $a_2 \to a_1$ steering $\mathcal{G}_{\mathrm{B}}$ also vanishes while the entanglement still exists, as shown in Figs. 2(d). It proves again that steering is a nonclassical correlation that is stronger than entanglement. As shown in Figs. 2(b) and 2(c), one-way $a_2 \to a_1$ steering can be achieved under appropriate parameter conditions. Its most promising potential application is that it provides security in one-sided device-independent quantum key distribution,[59–62] where the measurement apparatus of only one party is untrusted.

Figure 3 shows the intracavity entanglement E_{N} (black solid line), the intracavity steering $\mathcal{G}_{\mathrm{A}}$ (red dashed line), $\mathcal{G}_{\mathrm{B}}$ (blue dot-dashed line) and the steering asymmetry $|\mathcal{G}_{\mathrm{A}} - \mathcal{G}_{\mathrm{B}}|$ (green dotted line) versus cavity loss rate ratio κ_1/κ_2 for different normalized detunings Δ/Ω: (a) $\Delta/\Omega = -0.7$, (b) $\Delta/\Omega = -0.5$, (c) $\Delta/\Omega = -0.4$, (d) $\Delta/\Omega = -0.1$. The other parameters are the same as in Fig. 2. The cavity loss rate ratio κ_1/κ_2 determines the asymmetry of the system. It can be seen that the entanglement and the steering all drop rapidly with the increase of κ_1/κ_2 and the $a_1 \to a_2$ steering $\mathcal{G}_{\mathrm{A}}$ usually vanishes earlier than the $a_2 \to a_1$ steering $\mathcal{G}_{\mathrm{B}}$. Therefore there is a situation where there is only one-way $a_2 \to a_1$ steering. Taking Fig. 3(a) as an example ($\Delta/\Omega = -0.7$), both $\mathcal{G}_{\mathrm{A}}$ and $\mathcal{G}_{\mathrm{B}}$ are greater than zero in the region of $0 < \kappa_1/\kappa_2 < 3.2$. This means that two-way EPR steering can be obtained. When

$3.2 < \kappa_1/\kappa_2 < 7$, $\mathcal{G}_A = 0$ and $\mathcal{G}_B > 0$ and it means one-way $a_2 \to a_1$ steering. For $\kappa_1/\kappa_2 > 7$, $\mathcal{G}_A = 0$ and $\mathcal{G}_B = 0$, which indicates that there is no-way quantum steering between two cavity modes. When $\Delta/\Omega = -0.1$, as shown in Fig. 3(d), $\mathcal{G}_A = 0$ and $\mathcal{G}_B = 0$ while the entanglement still exists. This illustrates that the quantum steering is more fragile than the entanglement against the cavity loss rate ratio. We can control the normalized detuning Δ/Ω and cavity loss rate ratio κ_1/κ_2 to obtain large one-way steering while retaining a relatively high amount of entanglement.

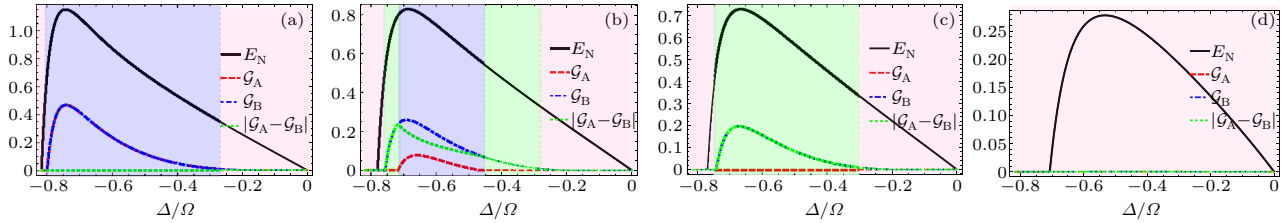


Fig. 2. The intracavity entanglement E_N (black solid line), the intracavity steering $\mathcal{G}_A$ (red dashed line), $\mathcal{G}_B$ (blue dot-dashed line) and the steering asymmetry $|\mathcal{G}_A - \mathcal{G}_B|$ (green dotted line) versus the normalized detuning Δ/Ω for different cavity loss rate ratios κ_1/κ_2: (a) $\kappa_1/\kappa_2 = 1$, (b) $\kappa_1/\kappa_2 = 3$, (c) $\kappa_1/\kappa_2 = 4$, (d) $\kappa_1/\kappa_2 = 16$. The other parameters are $\gamma_1 = \gamma_2 = 1$, $\kappa_2 = 0.1$, $g_1\sqrt{N} = g_2\sqrt{N} = 5$. In order to show the steering directivity clearly, we use the pink area to represent the presence of no-way steering, the green area to the presence of one-way $a_2 \to a_1$ steering and the purple area to the presence of two-way steering.

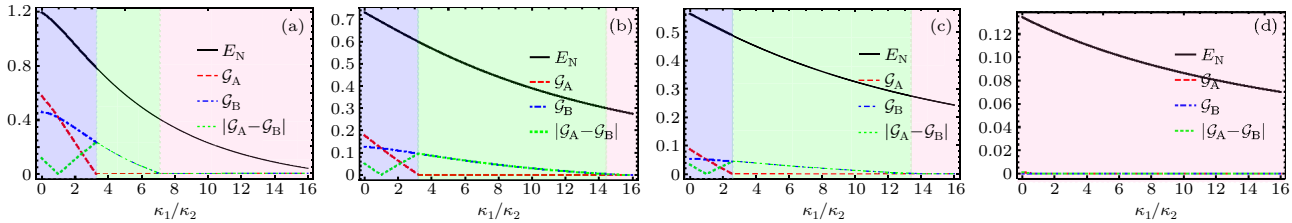


Fig. 3. The intracavity entanglement E_N (black solid line), the intracavity steering $\mathcal{G}_A$ (red dashed line), $\mathcal{G}_B$ (blue dot-dashed line) and the steering asymmetry $|\mathcal{G}_A - \mathcal{G}_B|$ (green dotted line) versus cavity loss rate ratio κ_1/κ_2 for different normalized detunings Δ/Ω: (a) $\Delta/\Omega = -0.7$, (b) $\Delta/\Omega = -0.5$, (c) $\Delta/\Omega = -0.4$, (d) $\Delta/\Omega = -0.1$. The other parameters are the same as in Fig. 2. The area colors have the same meaning as in Fig. 2.

To understand the internal mechanisms more clearly, we introduce a pair of Bogoliubov modes b_1 and b_2, which are unitary transformations of the cavity modes a_1 and a_2 with a two-mode squeezed operator, respectively,

$$\begin{aligned} b_1 &= S(r)a_1S^\dagger(r) = a_1\cosh r + a_2^\dagger \sinh r, \\ b_2 &= S(r)a_2S^\dagger(r) = a_2\cosh r + a_1^\dagger \sinh r, \end{aligned} \tag{14}$$

where $S(r) = \exp(ra_1a_2 - ra_1^\dagger a_2^\dagger)$ with the squeezing parameter $r = \tanh^{-1}\frac{|\sin\theta|}{1+\sin\theta}$. The Hamiltonian in Eq. (7) can be rewritten as

$$H_I' = \hbar\sqrt{g_a^2 - g_b^2}(b_1\sigma_{+0} + b_2\sigma_{-0}) + \text{H.c.}, \tag{15}$$

with $g_a = -g\cos^2\theta/2$, $g_b = g\sin\theta(1-\sin\theta)/2$ by assuming $g_1 = g_2 = g$. Physically, this Hamiltonian implies that the absorption of Bogoliubov modes $b_{1,2}$ is accompanied by the transitions $|0\rangle \to |\pm\rangle$. There are two dissipation channels to generate nonclassical states. If the steady-state population of state $|0\rangle$ is larger than that of states $|\pm\rangle$, i.e., $N_0 > N_\pm$, the dissipation processes are dominant over the amplification, giving rise to the suppression of quantum fluctuations. That is to say that the dressed atoms can be exploited to cool the Bogoliubov modes b_1 and b_2 to near ground states in a long enough time. The joint ground state of b_1 and b_2 is a two-mode squeezed vacuum state of the cavity modes a_1 and a_2, which can be checked by

$$b_j[S(r)|00\rangle_{a_1a_2}] = S(r)a_jS^\dagger(r)S(r)|00\rangle_{a_1a_2} = 0. \tag{16}$$

4. Output steering and entanglement spectra

Here we analyze the quantum correlations outside the two-mode cavity. The quantum Langevin equations can be solved in Fourier space. We define the Fourier-transformed operators by $a_j(\omega) = \int_{-\infty}^{+\infty} a_j(t)\,e^{i\omega t}\,dt$, $a_j^\dagger(\omega) \equiv \int_{-\infty}^{+\infty} a_j^\dagger(t)\,e^{i\omega t}\,dt = (a_j^\dagger)(\omega)$, $(j = 1, 2)$. The input noise correlation reads $\langle a_{j,\text{in}}(\omega)a_{j',\text{in}}^\dagger(\omega')\rangle = 2\pi\delta_{jj'}\delta(\omega+\omega')$ in the frequency domain. We find that the linear relation between output and input fields $\psi_{\text{out}}(\omega) = \boldsymbol{B}(\omega)\psi_{\text{in}}(\omega)$ can be found by the input–output relations[56] $a_{j,\text{out}}(t) = a_{j,\text{in}}(t) + \sqrt{\kappa_j}a_j(t)$, in a scattering matrix, $\boldsymbol{B}(\omega) = \sqrt{\boldsymbol{Q}}(\boldsymbol{R} + i\omega\boldsymbol{I})^{-1}\sqrt{\boldsymbol{Q}} + \boldsymbol{I}$. The input noise correlations $\Phi_{\text{in}}(\omega,\omega') = \langle\psi_{\text{in}}(\omega)\otimes\psi_{\text{in}}^{\text{T}}(\omega')\rangle$ are scattered into $\Phi_{\text{out}}(\omega,\omega') = \langle\psi_{\text{out}}(\omega)\otimes\psi_{\text{out}}^{\text{T}}(\omega')\rangle = \boldsymbol{B}(\omega)\Phi_{\text{in}}(\omega,\omega')\boldsymbol{B}^{\text{T}}(\omega')$. Then we can obtain[57,58]

$$\begin{aligned} n_j(\omega) &= \int_{-\infty}^{+\infty} e^{-i\omega t}\langle\hat{a}_{j,\text{out}}^\dagger(t)\hat{a}_{j,\text{out}}(0)\rangle, \\ n_x(\omega) &= \int_{-\infty}^{+\infty} e^{i\omega t}\langle\hat{a}_{1,\text{out}}(t)\hat{a}_{2,\text{out}}(0)\rangle, \end{aligned} \tag{17}$$

where $n_1(\omega)$ and $n_2(\omega)$ represent the output spectra for the a_1 and a_2 modes, respectively, and $n_x(\omega)$ represents the correlation between the ω component in the $a_{1,\text{out}}(t)$ mode and the $-\omega$ component in the $a_{2,\text{out}}(t)$ mode. Next we analyze the entanglement spectra between $a_{1,\text{out}}(\omega)$ and $a_{2,\text{out}}(-\omega)$. The entanglement of the system can be easily computed numerically using the covariance matrix and the definition of logarithmic

negativity. In order to analyze the output quantum correlation more clearly, we map the output state into a two-mode squeezed thermal state. Then, combining with Eqs. (11)–(13), we can plot the entanglement and quantum steering of the output fields.

Figure 4 shows the output entanglement $E_{\rm N}(0)$ (black solid line), the output steering $\mathcal{G}_{\rm A}(0)$ (red dashed line), $\mathcal{G}_{\rm B}(0)$ (blue dot-dashed line) and the steering asymmetry $|\mathcal{G}_{\rm A}(0)-\mathcal{G}_{\rm B}(0)|$ (green dotted line) at zero frequency versus the normalized detuning Δ/Ω for different cavity loss rate ratios κ_1/κ_2: (a) $\kappa_1/\kappa_2=1$, (b) $\kappa_1/\kappa_2=3$, (c) $\kappa_1/\kappa_2=8$, (d) $\kappa_1/\kappa_2=15$. The other parameters are $\gamma_1=\gamma_2=1$, $\kappa_2=0.1$, $g_1\sqrt{N}=g_2\sqrt{N}=1$. With the increase of the normalized detuning Δ/Ω, the output entanglement and steering first increase and then decrease. When increasing the cavity loss rate κ_1, the maximal values of entanglement and steering decrease gradually. These features are similar to the intracavity fields. However, unlike the intracavity steering, the direction of the output steering can be changed by adjusting the normalized detuning. Taking Fig. 4(b) as an example, in the region of $-0.76<\Delta/\Omega<-0.68$, there is one-way $a_2\to a_1$ EPR steering. For $-0.68<\Delta/\Omega<-0.5$, two-way EPR steering occurs. In the region of $-0.5<\Delta/\Omega<-0.3$, one-way $a_1\to a_2$ EPR steering arises. When $\kappa_1/\kappa_2=8$, as shown in Fig. 4(c), two-way EPR steering disappears and the range of one-way quantum steering becomes larger. Therefore, the output fields have more abundant quantum steering phenomena than the intracavity fields.

Figure 5 shows the output entanglement $E_{\rm N}(0)$ (black solid line), the output steering $\mathcal{G}_{\rm A}(0)$ (red dashed line), $\mathcal{G}_{\rm B}(0)$ (blue dot-dashed line) and the steering asymmetry $|\mathcal{G}_{\rm A}(0)-\mathcal{G}_{\rm B}(0)|$ (green dotted line) at zero frequency versus cavity loss rate ratio κ_1/κ_2 for different normalized detunings Δ/Ω: (a) $\Delta/\Omega=-0.77$, (b) $\Delta/\Omega=-0.6$, (c) $\Delta/\Omega=-0.48$, (d) $\Delta/\Omega=-0.1$. The other parameters are the same as in Fig. 4. It can be seen that the entanglement and the steering first increase and then decrease with the increase of κ_1/κ_2. The variation trend is different from that of intracavity fields. As shown in Fig. 5(b), one-way $a_2\to a_1$ EPR steering can be obtained in the region of $0<\kappa_1/\kappa_2<0.43$ and $5.38<\kappa_1/\kappa_2<15$. For $0.43<\kappa_1/\kappa_2<5.38$, there is two-way EPR steering. When $\Delta/\Omega=-0.48$, as shown in Fig. 5(c), one-way $a_1\to a_2$ EPR steering can be achieved in the region of $1.12<\kappa_1/\kappa_2<9.24$. Therefore, the direction of the output steering can be controlled by adjusting the normalized detuning Δ/Ω and cavity loss rate ratio κ_1/κ_2.

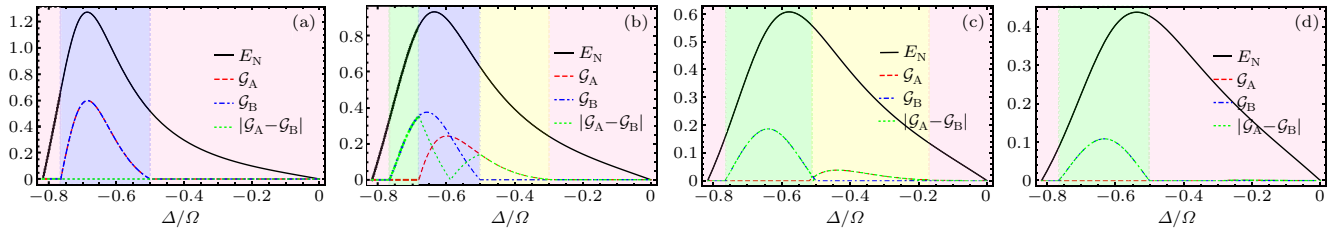


Fig. 4. The output entanglement $E_{\rm N}(0)$ (black solid line), the output steering $\mathcal{G}_{\rm A}(0)$ (red dashed line), $\mathcal{G}_{\rm B}(0)$ (blue dot-dashed line) and the steering asymmetry $|\mathcal{G}_{\rm A}(0)-\mathcal{G}_{\rm B}(0)|$ (green dotted line) at zero frequency versus the normalized detuning Δ/Ω for different cavity loss rate ratios κ_1/κ_2: (a) $\kappa_1/\kappa_2=1$, (b) $\kappa_1/\kappa_2=3$, (c) $\kappa_1/\kappa_2=8$, (d) $\kappa_1/\kappa_2=15$. The other parameters are $\gamma_1=\gamma_2=1$, $\kappa_2=0.1$, $g_1\sqrt{N}=g_2\sqrt{N}=1$. The yellow area represents the presence of one-way $a_1\to a_2$ steering. The other colors have the same meanings as in Fig. 2.

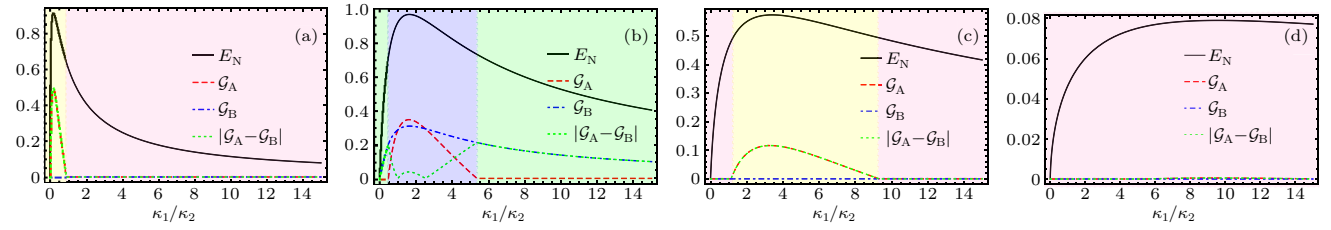


Fig. 5. The output entanglement $E_{\rm N}(0)$ (black solid line), the output steering $\mathcal{G}_{\rm A}(0)$ (red dashed line), $\mathcal{G}_{\rm B}(0)$ (blue dot-dashed line) and the steering asymmetry $|\mathcal{G}_{\rm A}(0)-\mathcal{G}_{\rm B}(0)|$ (green dotted line) at zero frequency versus cavity loss rate ratio κ_1/κ_2 for different normalized detunings Δ/Ω: (a) $\Delta/\Omega=-0.77$, (b) $\Delta/\Omega=-0.6$, (c) $\Delta/\Omega=-0.48$, (d) $\Delta/\Omega=-0.1$. The other parameters are the same as in Fig. 4. The colors have the same meaning as in Fig. 4.

5. Conclusion

In conclusion, we have used a four-wave mixing process to generate asymmetric EPR steering in a three-level Λ-type atomic ensemble. One-way quantum steering of both the intracavity fields and the output fields is achieved. Furthermore, we find that the output fields have more abundant quantum steering phenomena than the intracavity fields. The direction of the output steering can be switched by adjusting the normalized detuning and the cavity damping rates. However, the intracavity fields only have one-way $a_2\to a_1$ steering. The asymmetric quantum steering based on reservoir dissipation is robust against environmental noise. This is an experimentally feasible scheme, which has potential applications in quantum information tasks for quantum secret sharing protocols.

Appendix A

The damping rates in terms of the dressed states are given as

$$\gamma_{0+}=\gamma_{0-}=A^4(\gamma_1+\gamma_2),\ \ \gamma_{+0}=\frac{1}{2}E^2\left(C^2\gamma_1+F^2\gamma_2\right),$$
$$\gamma_{-0}=\frac{1}{2}E^2(F^2\gamma_1+C^2\gamma_2),\ \ \gamma_{+-}=C^2(A^2\gamma_1+E^2\gamma_2),$$
$$\gamma_{-+}=A^2(F_2\gamma_1+C^2\gamma_2),\ \ \gamma_{\rm ph}^{0+}=2A^2E(C\gamma_1-F\gamma_2),$$
$$\gamma_{\rm ph}^{0-}=-2A^2E(F\gamma_1-C\gamma_2),\ \ \gamma_{\rm ph}^{+-}=A^4(\gamma_1+\gamma_2),$$
$$\gamma_{\rm c1}=-A^2E(F\gamma_1-C\gamma_2),\ \ \gamma_{\rm c2}=A^2E(C\gamma_1-F\gamma_2),$$
$$\Gamma_1=2\gamma_{\rm ph}^{0+}+\frac{1}{2}(\gamma_{\rm ph}^{0-}+\gamma_{\rm ph}^{+-})+\gamma_{0+}+\gamma_{+0}+\gamma_{-0}+\gamma_{-+},$$
$$\Gamma_2=2\gamma_{\rm ph}^{0-}+\frac{1}{2}(\gamma_{\rm ph}^{0+}+\gamma_{\rm ph}^{+-})+\gamma_{+0}+\gamma_{0-}+\gamma_{-0}+\gamma_{+-},$$

where $A=\frac{\cos\theta}{\sqrt{2}}$, $C=\frac{1+\sin\theta}{2}$, $E=\sin\theta$, $F=\frac{1-\sin\theta}{2}$.

Acknowledgment

Project supported by Wuhan Donghu University Youth Foundation of Natural science (Grant No. 2022dhzk009).

References

[1] Einstein A, Podolsky B and Rosen N 1935 *Phys. Rev.* **47** 777
[2] Schrödinger E 1935 *Mathematical Proceedings of the Cambridge Philosophical Society* **31** 555
[3] Wiseman H M, Jones S J and Doherty A C 2007 *Phys. Rev. Lett.* **98** 140402
[4] Uola R, Costa A C S, Nguyen H C and Gühne O 2020 *Rev. Mod. Phys.* **92** 015001
[5] Wollmann S, Walk N, Bennet A J, Wiseman H M and Pryde G J 2016 *Phys. Rev. Lett.* **116** 160403
[6] Jones S J, Wiseman H M and Doherty A C 2007 *Phys. Rev. A* **76** 052116
[7] Nicolas B, Daniel C, Stefano P, Valerio S and Stephanie W 2014 *Rev. Mod. Phys.* **86** 419
[8] Vedral V, Plenio M B, Rippin M A and Knight P L 1997 *Phys. Rev. Lett.* **78** 2275
[9] Joseph B, Tamás V, Marco T Q and Nicolas B 2014 *Phys. Rev. Lett.* **112** 200402
[10] Qin Z Z, Deng X W, Tian C X, Wang M H, Su X L, Xie C D and Peng K C 2017 *Phys. Rev. A* **95** 052114
[11] Chen S L, Costantino B, Yeong C L and Chen Y N 2018 *Phys. Rev. A* **98** 042127
[12] He Q Y, Laura R Z, Gerardo A and Margaret R D 2015 *Phys. Rev. Lett.* **115** 180502
[13] Osorio C I, Bruno N, Sangouard N, Zbinden H, Gisin N and Thew R T 2012 *Phys. Rev. A* **86** 023815
[14] Jaeyoon C, Dimitris G A and Sougato B 2008 *Phys. Rev. A* **78** 022323
[15] Cavalcanti E G, Jones S J, Wiseman H M and Reid M D 2009 *Phys. Rev. A* **80** 032112
[16] Walborn S P, Salles A, Gomes R M, Toscano F and Souto Ribeiro P H 2011 *Phys. Rev. Lett.* **106** 130402
[17] Guhne O L and Lewenstein M 2004 *Phys. Rev. A* **70** 022316
[18] Liu S, Mu L Z and Fan H 2015 *Phys. Rev. A* **91** 042133
[19] Kogias I, Lee A R, Ragy S, and Adesso G 2015 *Phys. Rev. Lett.* **114** 060403
[20] Wang L, Lv S C and Jing J T 2017 *Opt. Exp.* **25** 17457
[21] Cavalcanti D and Skrzypczyk P 2019 *Phys. Rev. A* **93** 052112
[22] Armstrong S, Wang M Teh R Y, Gong Q H, He Q Y, Janousek J, Bachor H A, Reid M D and Lam P K 2015 *Nat. Phys.* **11** 167
[23] Deng X W, Xiang Y, Tian C X, Adesso G, He Q Y, Gong Q H, Su X L, Xie C D and Peng K C 2017 *Phys. Rev. Lett.* **118** 230501
[24] Liu Y, Zheng K M, Kang H J, Han D M, Wang M H, Zhang L J, Su X L and Peng K C 2022 *npj Quantum Inf.* **8** 38
[25] Deng X, Liu Y, Wang M H, Su X L and Peng K C 2021 *npj Quantum Inf.* **7** 65
[26] Smith D H, Gillett G, de Almeida M P, Branciard C, Fedrizzi A, Weinhold T J, Lita A, Calkins B, Gerrits T, Wiseman H M, Nam S W and White A G 2012 *Nat. Commun.* **3** 625
[27] Händchen V, Eberle T, Steinlechner S, Samblowski A, Franz T, Werner R F and Schnabel R 2012 *Nat. Photon.* **6** 596
[28] He Q Y, Gong Q H and Reid M D 2015 *Phys. Rev. Lett.* **114** 060402
[29] Xiao Y, Ye X J, Sun K, Xu J S, Li C F and Guo G C 2017 *Phys. Rev. Lett.* **118** 140404
[30] Zoller P, Marte M and Walls D F 1987 *Phys. Rev. A* **35** 198
[31] Rebić S, Vitali D, Ottaviani C, Tombesi P, Artoni M, Cataliotti F and Corbalán R 2004 *Phys. Rev. A* **70** 032317
[32] Sowik K, Filter R, Straubel J, Lederer F and Rockstuhl C 2013 *Phys. Rev. B* **88** 195414
[33] Johnson W R, Guo D S, Idrees M and Sapirstein J 1985 *Phys. Rev. A* **32** 2093
[34] Noh H R and Moon H S 2015 *Phys. Rev. A* **92** 013807
[35] Shen L T, Chen X Y, Yang Z B, Wu H Z and Zheng S B 2011 *Phys. Rev. A* **84** 064302
[36] Rao S, Hu X M, Li L C and Xu J 2016 *J. Phys. B: At. Mol. Opt. Phys.* **49** 225502
[37] Xu j, Wang F and Ge J 2018 *Ann. Phys.* **398** 24
[38] Tan H T and Sun L H 2015 *Phys. Rev. A* **92** 063812
[39] He Q Y, Ficek Z 2014 *Phys. Rev. A* **89** 022332
[40] Dabrowski M, Mazelanik M, Parniak M, Leszczyński A, Lipka M and Wasilewski W 2018 *Phys. Rev. A* **98** 042126
[41] Liu Y, Yin C, Yu X, Li F, Zhang Y P and He Q Y 2019 *Opt. Express* **27** 33070
[42] Zhong W X, Cheng G L and Hu X M 2017 *Opt. Express* **25** 11584
[43] Lawrie B J, Evans P G and Pooser R C 2013 *Phys. Rev. Lett.* **110** 156802
[44] Qin Z Z, Cao L M, Wang H L, Marion A M, Zhang W P and Jing J T 2014 *Phys. Rev. Lett.* **113** 023602
[45] Pooser R C, Savino N, Batson E, Beckey J L, Garcia J and Lawrie B J 2020 *Phys. Rev. Lett.* **124** 230504
[46] Braunstein D and Shuker R 2001 *Phys. Rev. A* **64** 053812
[47] Kreibich M, Main J and Wunner G 2012 *Phys. Rev. A* **86** 013608
[48] Gardiner C W and Zoller P 2000 *Quantum Noise* 2nd edn (Berlin: Springer-Verlag) pp. 15–20
[49] Scully M O and Zubairy M S 1997 *Quantum Optics* (New York: Cambridge University Press) pp. 20–30
[50] Routh E J 1877 *A treatise on the stability of a given state of motion* (London: Macmillan) pp. 12–14
[51] Hurwitz A 1895 *Math Ann.* **46** 273
[52] DeJesus E X and Kaufman C 1987 *Phys. Rev. A* **35** 5288
[53] Vidal G and Werner R F 2002 *Phys. Rev. A* **65** 032314
[54] Adesso G, Serafini A and Illuminati F 2004 *Phys. Rev. A* **70** 022318
[55] Plenio M B 2005 *Phys. Rev. Lett.* **95** 090503
[56] Aiello A 2000 *Phys. Rev. A* **62** 063813
[57] Deng Z J, Yan X B, Wang Y D and Wu C W 2016 *Phys. Rev. A* **93** 033842
[58] Deng Z J, Habraken S J and Marquardt F 2016 *New J. Phys.* **18** 063022
[59] Opanchuk B, Arnaud L and Reid M D 2014 *Phys. Rev. A* **89** 062101
[60] Branciard C, Cavalcanti E G, Walborn S P, Scarani V and Wiseman H M 2012 *Phys. Rev. A* **85** 010301
[61] Gehring T, Händchen V, Duhme J, Furrer F, Franz T, Pacher C, Werner R F and Schnabel R 2015 *Nat. Commun.* **6** 8795
[62] Walk N, Hosseni S, Geng J, Thearle O, Haw J Y, Armstrong S, Assad S M, Janousek J, Ralph T C, Symul T, Wiseman H M and Lam P K 2016 *Optica* **3** 634